ICRC 2001

New calculation of radioactive secondaries in cosmic rays

I. V. Moskalenko[1,2]**, S. G. Mashnik**[3]**, and A. W. Strong**[4]

[1]NRC-NASA/Goddard Space Flight Center, Code 660, Greenbelt, MD 20771, U.S.A.
[2]Institute of Nuclear Physics, M. V. Lomonosov Moscow State University, 119 899 Moscow, Russia
[3]Theoretical Division, Los Alamos National Laboratory, Los Alamos, NM 97545, U.S.A.
[4]Max-Planck-Institut für extraterrestrische Physik, Postfach 1312, 85741 Garching, Germany

Abstract. We use a new version of our numerical model for particle propagation in the Galaxy to study radioactive secondaries. For evaluation of the production cross sections we use the Los Alamos compilation of all available experimental cross sections together with calculations using the improved Cascade-Exciton Model code CEM2k. Using the radioactive secondary ratios ^{26}Al/^{27}Al, ^{36}Cl/Cl, ^{54}Mn/Mn, we show how the improved cross-section calculations together with the new propagation code allow us to better constrain the size of the CR halo.

1 Introduction

In recent years, new and accurate data have become available in CR astrophysics; more CR experiments are planned for launch in several years that will tremendously increase the quality and accuracy of CR data making further progress dependent on detailed models. Data will continue to flow from the high resolution detectors on Ulysses, Advanced Composition Explorer (ACE) and Voyager space missions. Several high resolution space experiments will be in orbit in the nearest 2–3 years, e.g., PAMELA to measure antiprotons, positrons, electrons, and isotopes H through C over the energy range of 0.1 to 200 GeV, and Alpha Magnetic Spectrometer (AMS) to measure particle and nuclear spectra to TeV enegies.

Measurements of secondary stable and radioactive nuclei in CR provide basic information necessary to probe large-scale Galactic properties, such as the diffusion coefficient and halo size, as well as mechanisms and sites of CR acceleration. Meanwhile, the accuracy of many of the nuclear cross sections used in CR astrophysics is far behind the accuracy of CR measurements of the current missions, such as Ulysses, ACE, and Voyager, and clearly becomes a factor restricting further progress. The widely used semi-phenomenological systematics have typical uncertainties more than $\sim 50\%$, and

Correspondence to: imos@milkyway.gsfc.nasa.gov

can sometimes be wrong by an order of magnitude (Mashnik 2000 and references therein); this is reflected in the value of propagation parameters and leads to uncertainties in the interpretation.

We have previously described a numerical model for the Galaxy encompassing primary and secondary CR, γ-rays and synchrotron radiation in a common framework (Strong et al., 2000). Up to recently our GALPROP code handled 2 spatial dimensions, (R, z), together with particle momentum p. This was used as the basis for studies of CR reacceleration, the size of the halo, positrons, antiprotons, dark matter and the interpretation of diffuse continuum γ-rays.

The experience gained from the original version allowed us to design a new version of the model, entirely rewritten in C++, which incorporates essential improvements over the older model, and in which a 3-dimensional spatial grid can be employed. It is now possible to solve the full nuclear reaction network on the spatially resolved grid. We keep however a "2D" option since this is often a sufficient approximation and is much faster to compute than the full 3D case. The code can thus serve as a complete substitute for the conventional "leaky-box" or "weighted-slab" propagation models usually employed, with many associated advantages such as the correct treatment of radioactive nuclei, realistic gas and source distributions etc.

In this paper we show our preliminary calculations of the radioactive secondary ratios ^{26}Al/^{27}Al, ^{36}Cl/Cl, ^{54}Mn/Mn using the Los Alamos compilation of experimental cross sections together with calculations by the code CEM2k (recognized by the nuclear physics community as among the best in predictive power as compared with other similar available codes).

2 Model

The GALPROP models have been described in full detail elsewhere (Strong and Moskalenko, 1998). The results obtained with the new version of GALPROP have been dis-

cussed in a recent review (Strong and Moskalenko, 2001a), and the most recent updates are described in Strong and Moskalenko (2001b).

In the new version, apart from the option of a full 3D treatment, we have updated the cross-section code to include latest measurements and energy dependent fitting functions. The nuclear reaction network is built using the Nuclear Data Sheets. The beryllium and boron production was calculated using the authors' fits to major production cross sections C,N,O(p,x)Be,B. For the main channels of production of isotopes of Al, Cl, Mn we use all experimental data available to us from the T16 LANL compilation by Mashnik et al. (1998) and calculations using the improved version (Mashnik and Sierk, 2000) of the Cascade-Exciton Model (Gudima et al., 1983) code CEM2k renormalized to the data if necessary. This code employs sophisticated microphysics via Monte Carlo calculations and it is difficult to use it "on-line" with our propagation code; other cross sections are thus calculated using the Webber et al. (1990) (wnewtr.for of 1993) phenomenological approximation renormalized to the data where it exists. For this purpose we use our internal database consisting of more than 2000 points collected from sources published in 1969–1999. (Another option is to use code yieldx_011000.for by Silberberg and Tsao.) For calculation of the total inelastic cross sections we use the latest version of the code CROSEC (Barashenkov and Polanski, 1994).

The reaction network is solved starting at the heaviest nuclei (i.e. ^{64}Ni), solving the propagation equation, computing all the resulting secondary source functions, and proceeding to the nuclei with $A - 1$. The procedure is repeated down to $A = 1$. In this way all secondary, tertiary etc. reactions are automatically accounted for. To be completely accurate for all isotopes, e.g. for some rare cases of $\beta^{\pm}$-decay, the whole loop is repeated twice.

3   Production cross sections

Since the calculations with the modern nuclear codes are very time consuming we check the effect of the new cross sections only on the isotopes of Al, Cl, and Mn. The radioactive isotopes of these elements are the main astrophysical time clocks which together with stable secondary isotopes allow us to probe global Galactic CR properties, in particular the halo size.

For isotopes of these elements we have chosen only the main production channels to calculate most accurately. For ^{26}Al the main progenitors are ^{27}Al and ^{28}Si, that for ^{27}Al is ^{28}Si. For isotopes of Cl the main progenitor is ^{56}Fe, but the contribution of many lighter nuclei is equally important. In the case of Mn, the main progenitor is ^{56}Fe with significant contribution of other isotopes of Fe, except for ^{55}Mn where only ^{56}Fe is important.

The experimental data for comparison should be taken carefully. The experimental technique in the past (γ-spectrometry) did not allow for the individual partial cross section to be extracted. Those measured represent the cross section of all the
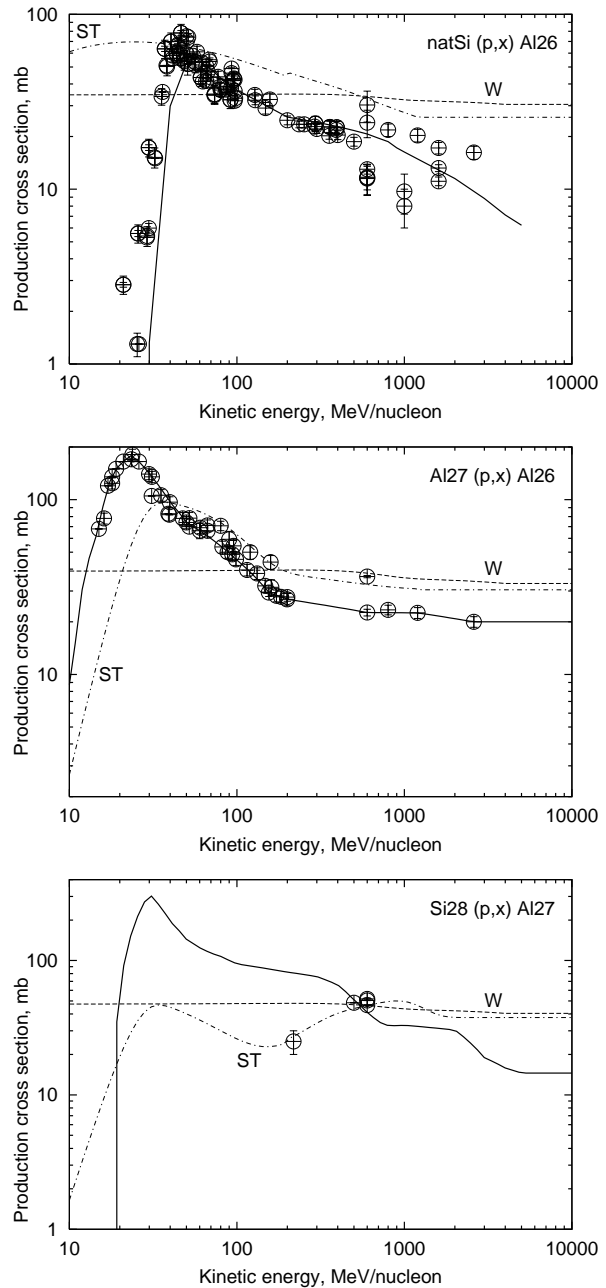

Fig. 1. Production cross sections of Al isotopes. The line coding: solid line – our adopted cross section, dashes – Webber et al. (1990) code (W), dash-dots – ST code. Data: T16 LANL compilation (Mashnik et al., 1998).

nuclear reaction chains ending at the particular isotope, i.e., almost always cumulative yields.

The simplest case is production of Al isotopes, however the abundant experimental measurements exist only for the natural Si $\rightarrow ^{26}$Al reaction. Natural silicon consists of 92% of ^{28}Si and the rest are isotopes ^{29,30}Si, 5% and 3% respectively (Anders and Grevesse, 1989). The measured cross section of the reaction ^{nat}Si$(p, x)^{26}$Al include also ^{nat}Si$(p, x)^{26}$Si, but the contribution is small.

Fig. 1 shows the experimental data for the inclusive re-

action $^{nat}\text{Si}(p,x)^{26}\text{Al}$, $^{27}\text{Al}(p,x)^{26}\text{Al}$, and $^{28}\text{Si}(p,x)^{27}\text{Al}$ together with calculations using CEM2k and Webber et al. (1990) and Silberberg and Tsao (ST) codes. In case of ^{nat}Si, calculations include weighted contribution of Si isotopes. Production of ^{26}Al is calculated as the sum of ^{26}Al and ^{26}Si production cross sections. In this particular case we use the data to renormalize the $^{28}\text{Si}(p,x)^{26}\text{Al}$ cross sections calculated by CEM2k. In case of the reaction $^{28}\text{Si}(p,x)^{27}\text{Al}$ ($+^{27}\text{Mg}$) we use a fit to the data, though the renormalized CEM2k model also works well above some tens of MeV.

4 Propagation of cosmic rays

Our preferred model for nuclei propagation is that with diffusive reacceleration. Though it has possible problems with secondary antiprotons and positrons (Moskalenko et al., 2001), it describes the spectra of nuclei and the stable secondary/primary nuclei ratios well. We thus will use the stochastic reacceleration model (SR-model) described in Moskalenko et al. (2001).

As in previous work, for each halo height z_h the model is adjusted to fit B/C, and the source abundances at the appropriate energy adjusted to agree with the relevant observed stable nuclei ratios; the fluxes of the radioactive isotopes are then computed. In this way the uncertainty in the denominator of the ratios is reduced. The heliospheric modulation is taken into account using the force-field approximation.

Fig. 2 shows the predicted interstellar and modulated B/C ratio compared with observations; the reacceleration reproduces the peak quite well.

The case of $^{26}\text{Al}/^{27}\text{Al}$ was the most uncertain giving the largest halo size in Strong and Moskalenko (2001a). From Fig. 1 it is clear that the discrepancy between the cross section calculations and data, which often exceeds a factor of 2, introduces a large error in the calculated ratio in CR.

Figs. 3-5 show $^{26}\text{Al}/^{27}\text{Al}$, $^{36}\text{Cl}/\text{Cl}$, $^{54}\text{Mn}/\text{Mn}$ ratios calculated with the new cross sections. For this calculation we used the half-life times of 0.87 Myr (^{26}Al), 0.31 Myr (^{36}Cl), 0.63 Myr (^{54}Mn). The ACE data points imply a halo size of a few kpc. The new limits derived, ^{26}Al: 3.5–6 kpc, ^{36}Cl: 4–15 kpc, ^{54}Mn: 3–7 kpc, are all consistent with our limits derived from Be: 1.5–6 kpc. The new limits include the error bars of the elemental abundance measurements from Ulysses (DuVernois and Thayer, 1996), to which we tune our propagated abundances. However, for isotopes of Al and Mn they are less important because there is only one major progenitor in each case.

Fig. 6 summarizes the halo size constraints obtained in this analysis. These estimates are based on the four radioactive isotopes by requiring consistency of the calculated ratio with the ACE data (Yanasak et al., 2000) and taking into account the error bars on both prediction and data. Also shown is the range derived in (Strong and Moskalenko, 2001a) employing the Webber et al. (1990) cross section code.

To remove uncertainty connected with elemental abundances errors, we propose in future to derive ratios of all isotopes
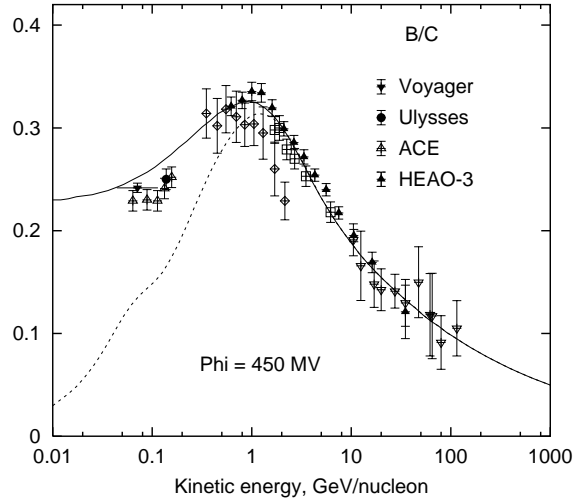

Fig. 2. B/C ratio as calculated for a model with reacceleration. Upper curve: modulated for 450 MV, lower curve: interstellar. Data: see Strong and Moskalenko (2001a).

of Al, Cl, Mn to the main progenitor, namely $^{26,27}\text{Al}/^{28}\text{Si}$, $^{35-37}\text{Cl}/^{56}\text{Fe}$, and $^{53-55}\text{Mn}/^{56}\text{Fe}$, not only the widely used $^{26}\text{Al}/^{27}\text{Al}$, $^{36}\text{Cl}/\text{Cl}$, and $^{54}\text{Mn}/\text{Mn}$ ratios. In case of Al and Mn isotopes this will virtually eliminate the need to tune the elemental abundances.

Some uncertainty still comes from modulation, while the experimental values for the ratios measured by ACE are rather accurate. However, because of the very flat ratio in the case of $^{54}\text{Mn}/\text{Mn}$ (below 1 GeV/nucleon) the modulation uncertainty is of minor importance.

The preliminary conclusion to be drawn from all radioactive nuclei is that, at least within the context of the present propagation model, $z_h = 4 - 6$ kpc based on the ACE data and Ulysses elemental abundances. This is consistent with our previous result $z_h = 3 - 7$ kpc (Strong and Moskalenko, 2001a) and supports our previous conclusion that the large dispersion between the isotopes is mostly due to cross-section inaccuracies.

References

Anders, E., and Grevesse, N., Geochim. Cosmochim. Acta, 53, 197–214, 1989.

Barashenkov, V. S., and Polanski, A., Communication JINR E2-94-417, Dubna, 1994.

Connell, J. J., Duvernois, M. A., and Simpson, J. A., Astrophys. J., 509, L97–L100, 1998.

DuVernois, M. A., Astrophys. J., 481, 241–252, 1997.

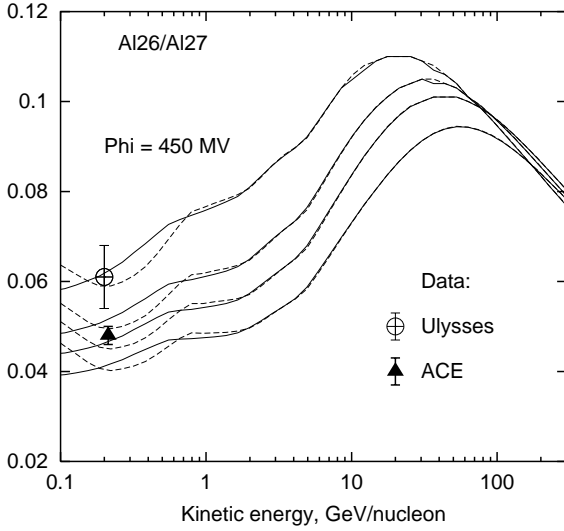DuVernois, M. A., and Thayer, M. R., Astrophys. J., 465, 982–984, 1996.

Fig. 3. ^{26}Al/^{27}Al ratio calculated for $z_h = 2, 4, 6, 10$ kpc (top to bottom). Solid curves – modulated, dashes – interstellar. Data: ACE – Yanasak et al. (2000), Ulysses – Simpson and Connell (1998).
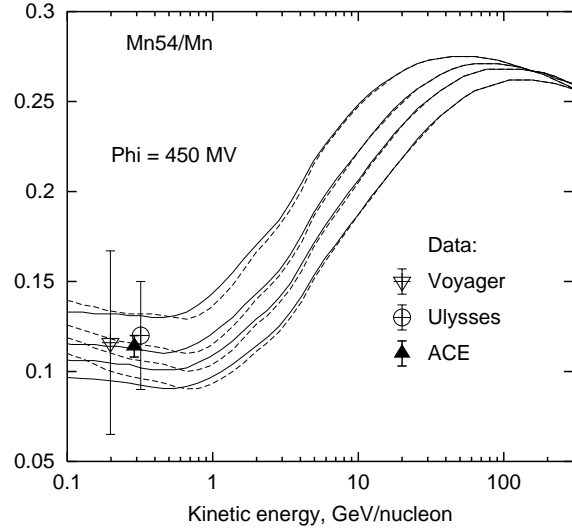

Fig. 5. ^{54}Mn/Mn ratio calculated for $z_h = 2, 4, 6, 10$ kpc (top to bottom). Solid curves – modulated, dashes – interstellar. Data: ACE – Yanasak et al. (2000), Ulysses – DuVernois (1997), Voyager – Lukasiak et al. (1997).
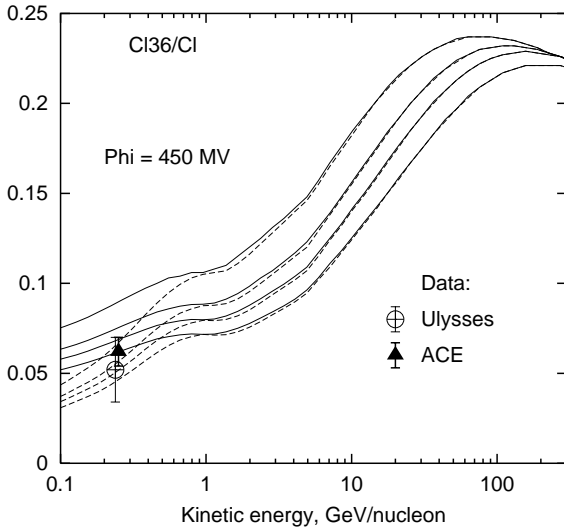

Fig. 4. ^{36}Cl/Cl ratio calculated for $z_h = 2, 4, 6, 10$ kpc (top to bottom). Solid curves – modulated, dashes – interstellar. Data: ACE – Yanasak et al. (2000), Ulysses – Connell et al. (1998).
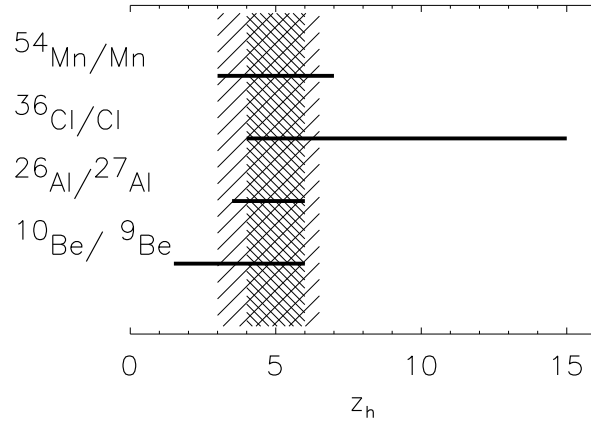

Fig. 6. Halo size limits as derived from the abundances of the four radioactive isotopes and ACE data. The ranges reflect errors in ratio measurements and source abundances. The dark shaded area indicates the range consistent with all ratios; for comparison the range from (Strong and Moskalenko, 2001a) is shown by light shading.

Gudima, K. K., Mashnik, S. G., and Toneev, V. D., Nucl. Phys. A, 401, 329–361, 1983.

Lukasiak, A., McDonald, F. B., and Webber, W. R., Astrophys. J., 488, 454–461, 1997.

Mashnik, S. G., astro-ph/0008382, 2000.

Mashnik, S. G., and Sierk, A.J., Proc. 4th Int. Topical Meeting on Nuclear Applications of Accelerator Technology (La Grange Park: ANS), 328–349, 2000; (nucl-th/0011064).

Mashnik, S. G., et al., Proc. 4th Workshop on Simulating Accelerator Radiation Environments, ed. Gabriel, T. A. (Oak Ridge: ORNL), 151–162, 1998; (nucl-th/9812071).

Moskalenko, I. V., et al., "Secondary antiprotons in cosmic rays", these proceedings, 2001.

Seo, E. S., and Ptuskin, V. S., Astrophys. J., 431, 705–714, 1994.

Simpson, J. A., and Connell, J. J., Astrophys. J., 497, L85–L88, 1998.

Strong, A. W., and Moskalenko, I. V., Astrophys. J., 509, 212–228, 1998.

Strong, A. W., and Moskalenko, I. V., Adv. Space Res., 27, 717–726, 2001a; (astro-ph/0101068).

Strong, A. W., and Moskalenko, I. V., "New developments in the GALPROP CR propagation model", these proceedings 2001b.

Strong, A. W., Moskalenko, I. V., and Reimer, O., Astrophys. J., 537, 763–784, 2000. Erratum: Ibid., 541, 1109, 2000.

Webber, W. R., Kish, J. C., and Schrier, D. A., Phys. Rev. C, 41, 566–571, 1990.

Yanasak, N. E., et al., Proc. ACE-2000 Symp., eds. Mewaldt, R. A., et al. (NY: AIP), AIP Conf. Proc., 528, 402–405, 2000.